

Eighth-Order Vacuum-Polarization Function Formed by Two Light-by-Light-Scattering Diagrams and its Contribution to the Tenth-Order Electron $g-2$

T. Aoyama,¹ M. Hayakawa,² T. Kinoshita,³ M. Nio,⁴ and N. Watanabe^{2,*}

¹*Institute of Particle and Nuclear Studies,*

High Energy Accelerator Research Organization (KEK), Tsukuba, 305-0801, Japan

²*Department of Physics, Nagoya University, Nagoya, Aichi 464-8602, Japan*

³*Laboratory for Elementary-Particle Physics,*

Cornell University, Ithaca, New York 14853, U.S.A.

⁴*Theoretical Physics Laboratory, Nishina Center, RIKEN, Wako, 351-0198, Japan*

(Dated: March 9, 2019)

Abstract

We have evaluated the contribution to the anomalous magnetic moment of the electron from six tenth-order Feynman diagrams which contain eighth-order vacuum-polarization function formed by two light-by-light scattering diagrams connected by three photons. The integrals are constructed by two different methods. In the first method the subtractive counter terms are used to deal with ultraviolet (UV) singularities together with the requirement of gauge-invariance. In the second method, the Ward-Takahashi identity is applied to the light-by-light scattering amplitudes to eliminate UV singularities. Numerical evaluation confirms that the two methods are consistent with each other within their numerical uncertainties. Combining the two results statistically and adding small contribution from the muons and/or tau leptons, we obtain $0.000\,399\,9\,(18)\,(\alpha/\pi)^5$. We also evaluated the contribution to the muon $g-2$ from the same set of diagrams and found $-1.263\,44\,(14)\,(\alpha/\pi)^5$.

PACS numbers: 13.40.Em, 14.60.Cd, 12.20.Ds, 06.20.Jr

*Electronic address: noriaki@eken.phys.nagoya-u.ac.jp

I. INTRODUCTION

The anomalous magnetic moment ($g-2$) of the electron has played the central role in testing the validity of quantum electrodynamics (QED) since its experimental and theoretical discovery in 1940's [1, 2].

The precision of $g-2$ measurements has been improved steadily in subsequent sixty years [3, 4]. The Harvard group recently succeeded in measuring the g value of the electron with a substantially reduced uncertainty by using a cylindrical Penning trap. Their measurements published in 2006 [5] and in 2008 [6] are

$$a_e(\text{HV06}) = 1\,159\,652\,180.85\,(76) \times 10^{-12} \quad [0.66\,\text{ppb}], \quad (1)$$

$$a_e(\text{HV08}) = 1\,159\,652\,180.73\,(28) \times 10^{-12} \quad [0.24\,\text{ppb}]. \quad (2)$$

Taking the presence of the muon and tau lepton into account the QED contribution to the electron $g-2$ can be written in the general form

$$a_e(\text{QED}) = A_1 + A_2(m_e/m_\mu) + A_2(m_e/m_\tau) + A_3(m_e/m_\mu, m_e/m_\tau), \quad (3)$$

where A_i can be expanded into power series in $\frac{\alpha}{\pi}$

$$A_i = A_i^{(2)} \left(\frac{\alpha}{\pi}\right) + A_i^{(4)} \left(\frac{\alpha}{\pi}\right)^2 + A_i^{(6)} \left(\frac{\alpha}{\pi}\right)^3 + \dots, \quad i = 1, 2, 3, \quad (4)$$

whose coefficients are finite calculable quantities, which is guaranteed by the renormalizability of QED. Thus far the coefficients up to the eighth-order have been calculated [7, 8, 9, 10, 11, 12, 13, 14, 15, 16, 17, 18, 19, 20]. The small but non-negligible corrections due to hadrons [21, 22, 23, 24] and weak interactions [25] are also known with sufficient precision.

Combining the experiment and the theory, one can determine the value of the fine structure constant α [6, 26, 27]

$$\alpha^{-1}(a_e) = 137.035\,999\,084\,(12)(37)(33) \quad [0.37\,\text{ppb}], \quad (5)$$

where the uncertainties come from numerical errors in the eighth-order term [12, 13], an educated guess of the tenth-order term [28], and the experiment (2), in that order. Note that, for the first time in three decades, the experimental uncertainty (0.33×10^{-7}) has been reduced to a value smaller than the combined theoretical uncertainty (0.39×10^{-7}). The

uncertainty of this α is about 20 times smaller than those of other independent methods, such as a Rb recoil velocity determination in an optical lattice [29] or a Cs recoil velocity in an atom interferometry [30, 31]. A new Cs measurement is now in progress, which is designed to obtain the value of α with the relative uncertainty 0.3 ppb [32]. Such forthcoming progress of the atomic physics experiments will enable us to check the validity of QED with the accuracy less than 0.1 ppb by examining consistency of various values of α .

Turning back to the electron $g-2$, we find that the largest theoretical uncertainty now comes from the tenth-order term $A_1^{(10)}$. Clearly an actual value, not an estimate, of this term is urgently needed. There are 12672 Feynman diagrams contributing to $A_1^{(10)}$. Our on-going effort to evaluate all of them has been reported in several articles [33, 34, 35, 36, 37, 38, 39, 40]. In this paper, we report the contribution from the diagrams belonging to the gauge-invariant set Set I(j). These diagrams contain the eighth-order vacuum-polarization diagram formed by two light-by-light scattering diagrams connected by three photons, which was constructed first time in this work. Although the Set I(j) consists of only six Feynman diagrams and it turns out to be numerically very small, it has features not found in other 12666 diagrams contributing to the tenth-order electron $g-2$. Thus it deserves a special treatment as is described in this paper.

The primary purpose of this paper is to report the contribution of the gauge-invariant set Set I(j) to the mass-independent term $A_1^{(10)}$ of the electron $g-2$. The contributions to $A_2^{(10)}$ from closed loops of electrons, muons and/or tau leptons are evaluated and reported separately in Sec. IV. Summing up all contributions, we obtained the tenth-order contribution from Set I(j)

$$\begin{aligned} a_e^{(10)}(\text{Set I(j)}) &= \left(A_1^{(10)}(\text{Set I(j)}) + A_2^{(10)}(m_e/m_\mu)(\text{Set I(j)}) \right) \left(\frac{\alpha}{\pi} \right)^5 \\ &= 0.000\,399\,9\,(18) \left(\frac{\alpha}{\pi} \right)^5. \end{aligned} \quad (6)$$

The contribution from the tau lepton is smaller than the uncertainty quoted here.

The contribution of Set I(j) to the muon $g-2$ can be obtained by replacing the external (or open) electron line by a muon line, keeping the internal fermion loops intact. The result

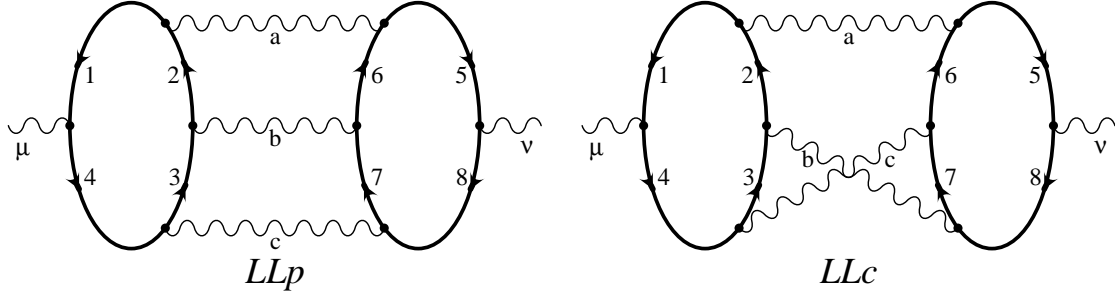


FIG. 1: Eighth-order vacuum-polarization diagrams LLp and LLc . There are two diagrams of LLp type and four diagrams of LLc type. When inserted into a photon line of the second-order vertex diagram, they give the tenth-order diagrams contributing to the lepton $g-2$ called Set I(j).

of numerical integration gives the mass-dependent term of the muon $g-2$

$$\begin{aligned}
 a_{\mu}^{(10)}(\text{Set I(j)}) &= \left(A_2^{(10)}(m_{\mu}/m_e)(\text{Set I(j)}) + A_2^{(10)}(m_{\mu}/m_{\tau})(\text{Set I(j)}) \right. \\
 &\quad \left. + A_3^{(10)}(m_{\mu}/m_e, m_{\mu}/m_{\tau})(\text{Set I(j)}) \right) \left(\frac{\alpha}{\pi} \right)^5 \\
 &= -1.263\,44\,(14) \left(\frac{\alpha}{\pi} \right)^5.
 \end{aligned} \tag{7}$$

The contribution from tau lepton is of order of the uncertainty quoted here.

In Sec. II we describe how to construct the eighth-order vacuum-polarization function of Set I(j). Three possible ways are considered. In Sec. III two of three methods are described in detail. The utility of the Ward-Takahashi identity applied to a vacuum-polarization diagram and a light-by-light scattering diagram is particularly emphasized. Once the vacuum-polarization function is constructed, its contribution to the tenth-order anomaly is easily calculated. The details of the numerical results are presented in Sec. IV. Sec. V is devoted to conclusion and discussion. Appendix A describes new features of the vacuum-polarization function for the diagrams of Set I(j) and also shows how to obtain its contribution to the magnetic moment which does not rely on the photon spectral function explicitly. An example of the structure of the integrand used in the Method C is shown in Appendix B.

II. EIGHTH-ORDER VACUUM-POLARIZATION DIAGRAMS WHICH CONSIST OF TWO LIGHT-BY-LIGHT-SCATTERING SUBDIAGRAMS CONNECTED BY THREE PHOTONS

Two approaches are found in the literature for dealing with the insertion of a vacuum-polarization diagram in the photon line of the second-order vertex diagram. One is to take advantage of the fact that such an insertion amounts to replacing the photon line by a sum of massive vector particles weighted by the spectral function, which is the absorptive part of the vacuum-polarization function. Another is to insert the vacuum-polarization function itself obtained by the Feynman-Dyson rules. The first method is very convenient if the spectral function is known exactly [41], or in good approximation [42]. In most cases where such a spectral function is not available, however, one is forced to choose the second approach. The tenth-order diagrams of Set I(j), which consist of eighth-order vacuum-polarization functions inserted into the second-order vertex diagram, belong to the latter. This approach was initially developed in Refs. [43, 44]. (See also Eqs. (5.6) and (5.8) of Ref. [45]). A more transparent and compact form is presented in [46]:

$$a^{(2+n)} = - \int_0^1 dy (1-y) \Pi^{(n)} \left(-\frac{y^2}{1-y} \right), \quad (8)$$

where $a^{(2+n)}$ stands for the $(2+n)$ th-order electron anomaly that is obtained from the second-order vertex diagram in which the renormalized n th-order vacuum-polarization function $\Pi^{(n)}$ is inserted. A derivation of Eq. (8) is given in Appendix A.

In the second approach the problem is thus reduced to an explicit construction of Π from the gauge-invariant set Set I(j) of Feynman diagrams. When twisted and flipped appropriately, two of the vacuum-polarization diagrams of Set I(j) (called *LLp*) are reduced to planar form with three uncrossed photons, and four of them (called *LLc*) have lower two of the photon lines crossed (see Fig. 1). Applying Feynman-Dyson rules formally to one of the *LLp*-type diagrams we obtain

$$\begin{aligned} \Pi_{LLp}^{\mu\nu}(q) = & (-1)^2 \frac{1}{(2\pi)^8} \left(\frac{\alpha}{\pi} \right)^4 \int d^4 l_1 \int d^4 l_2 \int d^4 l_3 \int d^4 l_4 \\ & \times \text{Tr} \left[\gamma^\mu \frac{1}{\not{p}_1 - m} \gamma^\alpha \frac{1}{\not{p}_2 - m} \gamma^\beta \frac{1}{\not{p}_3 - m} \gamma^\zeta \frac{1}{\not{p}_4 - m} \right] \frac{1}{p_a^2} \frac{1}{p_b^2} \frac{1}{p_c^2} \\ & \times \text{Tr} \left[\gamma^\nu \frac{1}{\not{p}_5 - m} \gamma_\alpha \frac{1}{\not{p}_6 - m} \gamma_\beta \frac{1}{\not{p}_7 - m} \gamma_\zeta \frac{1}{\not{p}_8 - m} \right], \quad (9) \end{aligned}$$

where each closed lepton loop contributes a factor -1 , p_i are linear combinations of loop momenta l_1, l_2, l_3, l_4 and external momentum q , which enters at the μ vertex and leaving at the ν vertex (see Fig. 1).

The second LLp -type diagram is obtained by reversing the direction of the arrow of lepton lines in the second trace of Eq. (9). By charge-conjugation invariance of QED it is equivalent to the first one. The LLc -type diagrams are obtained by exchanging γ_β and γ_ζ in the second trace of Eq. (9). All four diagrams of LLc -type are equivalent to each other.

Of course formal expressions such as Eq. (9) are UV-divergent and meaningless until they are regularized properly. We follow the standard procedure to extract physical information from the expression (9) and a similar one for LLc :

- (i) Make them convergent by the Pauli-Villars regularization of lepton loops and the Feynman cutoff of photon propagators.
- (ii) Renormalize them by subtractive renormalization, where subtraction integrals must be regularized in the same way as in (i).
- (iii) Remove the regularization terms from the final renormalized formula.

These steps ensure that individual integrals obtained are finite. However they still contain terms which are not gauge-invariant. These terms cancel out only after they are summed over the gauge-invariant set of Feynman diagrams. Some details of the steps are described in the following.

The integral (9) has eight UV-divergent subdiagrams, including itself. They are, namely, the light-by-light-scattering subdiagram L (formed by a closed loop of lepton lines 1, 2, 3, 4), another light-by-light-scattering subdiagram R (formed by a closed loop of lepton lines 5, 6, 7, 8), a sixth-order vertex diagram V (formed by lepton lines 1, 2, 3, 4, 6, 7 and photon lines a, b, c), another sixth-order vertex diagram W (formed by lepton lines 2, 3, 5, 6, 7, 8 and photon lines a, b, c), diagrams of the type (L in V) and (R in W), and the diagram itself that consists of all lepton lines 1, 2, 3, 4, 5, 6, 7, 8 and all photon lines a, b, c (see Fig. 2). One more type of UV-divergence caused by L and R together generates no terms which contribute to the anomaly. Thus it can be ignored.

UV divergences coming from L and R are only logarithmic and can be controlled by the Pauli-Villars regularization of the lepton loop. Control of UV divergences of V and W

requires Pauli-Villars regularization as well as Feynman cut-off of virtual photon momenta. In the latter, the photon propagator with momentum k is regularized as

$$\frac{1}{k^2 - \lambda^2} = - \int_{\lambda^2}^{\Lambda^2} dM^2 \frac{1}{(k^2 - M^2)^2} , \quad (10)$$

where the photon mass λ and the UV cut-off Λ are introduced temporarily and to be put to zero and infinity, respectively, in the end. Finally, we must control the UV divergence involving all lepton lines and all photon lines. It is important to note that this divergence cannot be controlled by Pauli-Villars regularizations of two closed lepton loops alone. The quadratic behavior of this divergence comes mostly from three photons working together, a novel feature encountered for the first time in the eighth-order vacuum polarization.

The sum $\Pi^{\mu\nu}(q)$ of all six diagrams, two of LLp type and four of LLc type, is gauge invariant and completely free of divergence after charge renormalization is carried out. However, in our numerical work which adopts the parametric integral formulation based on the topology of an individual Feynman diagram [47, 48], it is more convenient to deal with the diagrams LLp and LLc separately. This means that we must go one step backwards and explicitly carry out the renormalization of logarithmic divergence from light-by-light scattering sub-diagrams, etc., as well as the quadratic divergence from the vacuum-polarization diagram as a whole. The logarithmic divergence is very mild and its removal by renormalization can be handled within the numerical framework keeping the gauge-invariance rigorously.

The standard way to handle the quadratic UV divergence is to note that the Lorentz covariance dictates that $\Pi_{\mathcal{G}}^{\mu\nu}$, of either $\mathcal{G} = LLp$ or LLc , consists of two scalar functions $\Pi_{\mathcal{G}}^{(a)}(q^2)$ and $\Pi_{\mathcal{G}}^{(b)}(q^2)$:

$$\Pi_{\mathcal{G}}^{\mu\nu}(q) = g^{\mu\nu} \Pi_{\mathcal{G}}^{(a)}(q^2) + q^\mu q^\nu \Pi_{\mathcal{G}}^{(b)}(q^2) , \quad (11)$$

and note that $\Pi_{\mathcal{G}}^{\mu\nu}(q)$ has the dimension of square of momentum so that the quadratic divergence (which is proportional to the cut-off momentum squared) is confined to the term proportional to $g^{\mu\nu}$, or more precisely to the q -independent part of $\Pi_{\mathcal{G}}^{(a)}(q^2)$. Thus, if we write $\Pi_{\mathcal{G}}^{(a)}(q^2)$ as

$$\Pi_{\mathcal{G}}^{(a)}(q^2) = [\Pi_{\mathcal{G}}^{(a)}(q^2) - \Pi_{\mathcal{G}}^{(a)}(0)] + \Pi_{\mathcal{G}}^{(a)}(0) , \quad (12)$$

the term within the parentheses is free from the quadratic divergence.

As is well-known, gauge-invariance dictates that quadratic divergences in $\Pi_{\mathcal{G}}^{\mu\nu}(q)$ of the individual diagrams should disappear from the sum of the gauge-invariant set of the diagrams,

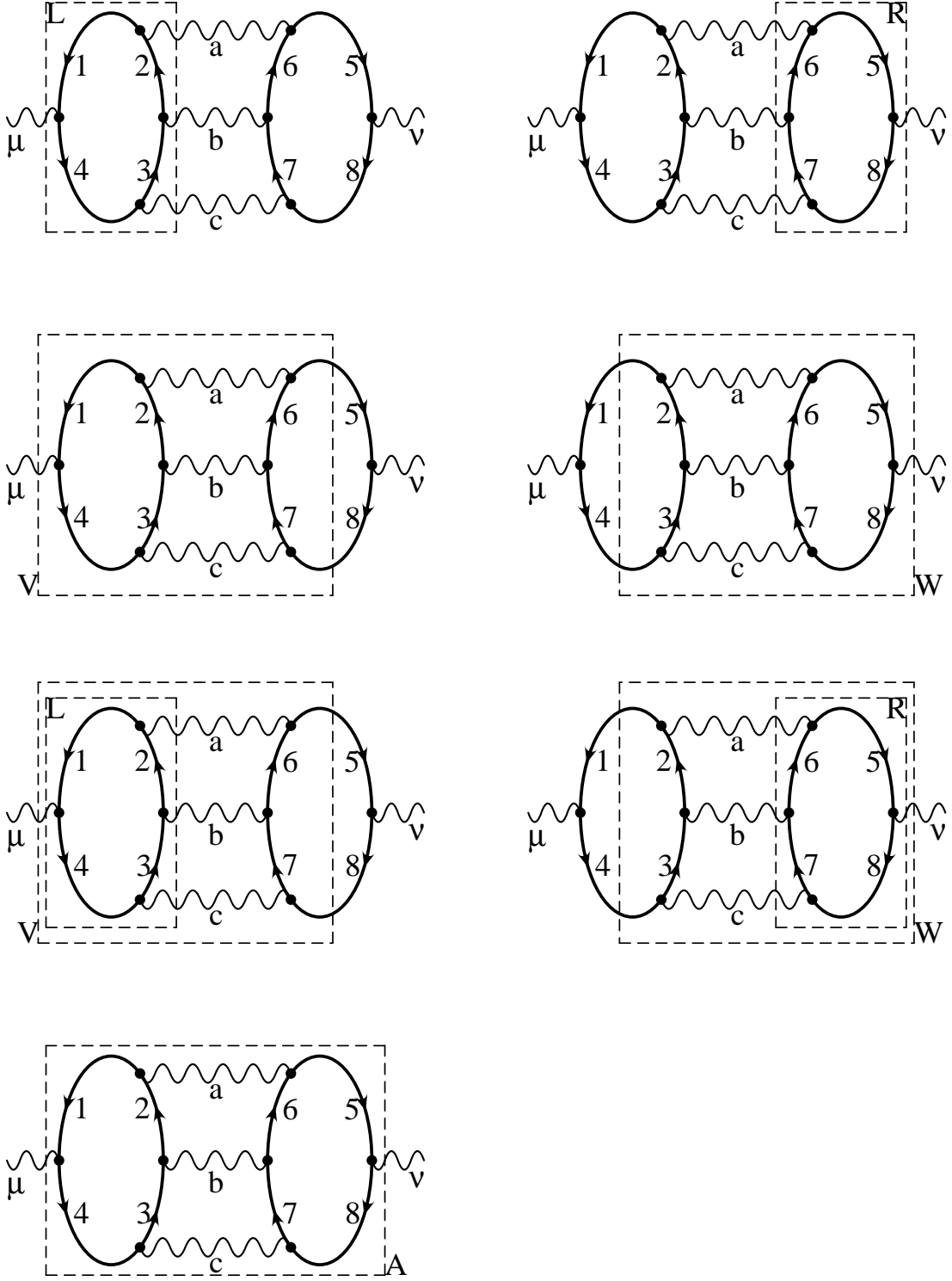


FIG. 2: Divergence structure of LLp . Subdiagrams are L , R , V , W , L in V , and R in W , and the whole diagram A of LLp .

and $\Pi^{\mu\nu}(q) \equiv 4\Pi_{LLp}^{\mu\nu} + 2\Pi_{LLc}^{\mu\nu}$ should satisfy the transversality condition

$$\Pi^{\mu\nu}(q) = (q^\mu q^\nu - q^2 g^{\mu\nu})\Pi^{(b)}(q^2). \quad (13)$$

The scalar function $\Pi^{(b)}(q^2) \equiv 2\Pi_{LLp}^{(b)}(q^2) + 4\Pi_{LLc}^{(b)}(q^2)$ defined by this equation is free from all subdiagram UV divergences. However it still has an overall UV divergence which must be removed by subtraction of $\Pi^{(b)}(0)$, which is nothing but charge renormalization.

These observations lead us to three possible methods for obtaining the renormalized (not yet gauge invariant) amplitude $\Pi_G(q^2)$, which is the LLp or LLc part of $\Pi^{(b)}(q^2) - \Pi^{(b)}(0)$. The first method is

Method A. Collect all terms of $\Pi^{\mu\nu}(q)$ which are coefficients of $q^\mu q^\nu$.

Another approach is to note that Eq. (13) implies

$$q_\lambda \Pi^{\lambda\nu}(q) = 0, \quad (14)$$

which is valid for arbitrary q . Differentiating this equation with respect to q_μ we obtain

$$\Pi^{\mu\nu}(q) = -q_\lambda \frac{\partial}{\partial q_\mu} \Pi^{\lambda\nu}(q), \quad (15)$$

in which one power of q is extracted explicitly. This has the effect of removing the quadratic UV divergence automatically. Thus, we can choose

Method B. Collect coefficients of $q^\mu q^\nu$ or those of $-g^{\mu\nu}q^2$ of $\Pi^{\mu\nu}$ from the right-hand side of Eq. (15).

Yet another approach is to start from the equation involving the second derivative of $\Pi^{\mu\nu}(q)$:

$$\Pi^{\mu\nu}(q) = \frac{1}{2} q_\lambda q_\sigma \frac{\partial}{\partial q_\mu} \frac{\partial}{\partial q_\nu} \Pi^{\lambda\sigma}(q), \quad (16)$$

which follows from Eq. (15) and

$$q_\lambda q_\sigma \Pi^{\lambda\sigma}(q) = 0, \quad (17)$$

and symmetry of $\Pi^{\mu\nu}$ in μ and ν . Thus we may also start from the following rule in which two powers of q are extracted explicitly:

Method C. Collect coefficients of $q^\mu q^\nu$ or those of $-g^{\mu\nu}q^2$ of $\Pi^{\mu\nu}$ from the right-hand side of Eq. (16).

It turns out that Method C has a distinct advantage over the other two. Not only the

quadratic divergence but also subdiagram logarithmic UV divergences, except for the one requiring charge renormalization, are eliminated as a consequence of the second derivative. Aside from this difference, however, Method A and Method B are equally useful and effective as Method C for carrying out numerical evaluation of the contribution of the Set I(j).

III. CONSTRUCTION OF THE VACUUM-POLARIZATION FUNCTION $\Pi(q^2)$

A. Parametric representation of $\Pi(q^2)$

Once the integral is made finite by regularization, we can safely deal with individual diagrams. In this article we adopt the method of parametric representation which has been successfully applied to similar problems [45]. We begin by replacing the numerator, e.g., of Eq. (9), by an operator

$$\begin{aligned} \mathcal{F} \equiv & \text{Tr} [\gamma^\mu (\not{D}_1 + m) \gamma^\alpha (\not{D}_2 + m) \gamma^\beta (\not{D}_3 + m) \gamma^\zeta (\not{D}_4 + m)] \\ & \times \text{Tr} [\gamma^\nu (\not{D}_5 + m) \gamma_\alpha (\not{D}_6 + m) \gamma_\beta (\not{D}_7 + m) \gamma_\zeta (\not{D}_8 + m)], \end{aligned} \quad (18)$$

where [49]

$$D_j^\mu = \frac{1}{2} \int_{m_j^2}^{\infty} dm_j^2 \frac{\partial}{\partial q_{j\mu}}, \quad (19)$$

and bring it in front of the momentum integration. (This may not be as straightforward as it sounds, and requires a more careful argument of Pauli-Villars regularization. But the end result is correct.) Then we combine all denominators with the help of Feynman parameters z_1, \dots, z_8 for leptons and z_a, z_b, z_c for photons:

$$\begin{aligned} & \frac{1}{p_a^2} \frac{1}{p_b^2} \frac{1}{p_c^2} \prod_{i=1}^8 \frac{1}{p_i^2 - m_i^2} \\ &= 10! \int (dz) \frac{1}{(\sum_{i=1}^8 z_i(p_i^2 - m_i^2) + z_a(p_a^2 - \lambda^2) + z_b(p_b^2 - \lambda^2) + z_c(p_c^2 - \lambda^2))^{11}}, \end{aligned} \quad (20)$$

where the photon mass λ is introduced temporarily, to be put to zero in the end.

The Feynman regularization for a photon propagator introduced in (10) modifies the unregularized expression (20) to

$$\begin{aligned} & \frac{1}{(\sum_{i=1}^8 z_i(p_i^2 - m_i^2) + z_a(p_a^2 - \lambda^2) + z_b(p_b^2 - \lambda^2) + z_c(p_c^2 - \lambda^2))^{11}} \\ &= -11 \int_{\lambda^2}^{\Lambda^2} dM^2 \frac{z_{abc}}{(\sum_{i=1}^8 z_i(p_i^2 - m_i^2) + z_a p_a^2 + z_b p_b^2 + z_c p_c^2 - z_{abc} M^2)^{12}}, \end{aligned} \quad (21)$$

where Λ is the UV cutoff and $z_{abc} = z_a + z_b + z_c$. Let us assume that this regularization is implicitly and always done. Now we can carry out the momentum integration and obtain

$$\begin{aligned} & \int d^4 l_1 \int d^4 l_2 \int d^4 l_3 \int d^4 l_4 \frac{1}{(\sum_{i=1}^8 z_i (p_i^2 - m_i^2) + z_a p_a^2 + z_b p_b^2 + z_c p_c^2 - z_{abc} \lambda^2)^{11}} \\ &= -\frac{(\pi^2 i)^4}{((11-1)!)/((11-9)!)} \int (dz) \frac{1}{U^2 V^3}, \end{aligned} \quad (22)$$

where

$$V = z_{1234} m^2 + z_{5678} m^2 + z_{abc} \lambda^2 - q^2 G, \quad (23)$$

$z_{1234} = z_1 + z_2 + z_3 + z_4$, etc., and

$$G = -z_1 A_1 + z_a A_a + z_5 A_5, \quad (24)$$

assuming that the photon momentum q enters the diagram at the vertex μ , goes through lepton line 1, photon line a , lepton line 5, and exits from the vertex ν . A_i is the scalar current associated with the line i [45]. Note that A_1 is defined assuming that the arrow of fermion line 1 is opposite to the direction of q , whereas the photon line a and fermion line 5 are in the same direction as q (see Fig. 1). (Actually, any continuous path of q is equivalent to that of (24), as far as the integral is made finite by regularization. Note that this may not be guaranteed for divergent integrals.) U is a Jacobian from the momentum space to the Feynman parameter space. (dz) stands for the eleven dimensional integration variables of Feynman parameters with the constraint that the sum of eleven Feynman parameters is unity. Although this integral is still logarithmically divergent, when it is regularized with the cut-off of Eq. (21), \mathcal{F} operation can be carried out correctly. (If necessary, we can introduce another cutoff parameter.)

Collecting all numerical factors and bringing \mathcal{F} back into the integral we obtain, for LLp ,

$$\begin{aligned} \Pi_{LLp}^{\mu\nu}(q) &= -(-1)^2 \frac{1}{(2\pi)^8} \left(\frac{\alpha}{\pi}\right)^4 (10!) \frac{(\pi^2 i)^4}{((11-1)!)/((11-9)!)} \int (dz) \mathcal{F} \frac{1}{U^2 V^3} \\ &= -\frac{2!}{2^8} \left(\frac{\alpha}{\pi}\right)^4 \int (dz) \mathcal{F} \frac{1}{U^2 V^3}. \end{aligned} \quad (25)$$

Before proceeding further we must carry out renormalization explicitly, following a well-established method. We mention here only few aspects that are specific to Set I(j).

The first point to note is that the renormalization constants for the sixth-order vertices V and W are actually zero for the gauge-invariant quantity $\Pi(q^2)$ by Furry's theorem since

there is no “self-energy” diagrams corresponding to V or W . However, they are nonvanishing for individual integrals, and must be subtracted explicitly from the unrenormalized integral. The leading logarithmic part of such a subtraction term can be readily obtained by the K -operation [45], in which the UV divergent part of the standard on-shell renormalization constant is used. However, in the case of Set I(j), it turns out to be better to construct the exact and full on-shell renormalization term which enables us to avoid the trouble of calculating the residual renormalization term separately.

Similarly, for the light-by-light-scattering amplitudes of L and R , we can avoid residual renormalization by defining the renormalization terms as the standard on-shell amplitudes defined with all its momenta *external* to it put to zero. The gauge invariant set of this light-by-light scattering amplitude is summed up to zero, which can also be shown by calculation with the dimensional regularization, hence no residual renormalization is needed.

The integrals obtained by the Method A and the Method B can be shown to be analytically identical using “Kirchhoff’s laws” on junctions and loops [45]. In the following we shall therefore consider only Method B and Method C.

B. More on Method B

We are now ready to consider Method B in detail. Let us write the integral for LLp symbolically, ignoring explicit multiple integration, as

$$\Pi = LSR, \quad (26)$$

where L and R are light-by-light-scattering diagrams introduced previously and S stands for the set of three photons connecting L and R . Then, the differentiation in Eq. (15) can be carried out as

$$\frac{\partial}{\partial q_\mu} \Pi = \left(\frac{\partial}{\partial q_\mu} L \right) SR + L \left(\frac{\partial}{\partial q_\mu} S \right) R + LS \left(\frac{\partial}{\partial q_\mu} R \right). \quad (27)$$

The first and third terms involve differentiation of the lepton propagators in the closed lepton loops while the second one is differentiation of the photon propagator. These differentiation can be carried out using the identities [45]

$$\frac{\partial}{\partial q_\mu} \frac{1}{\not{p} + \not{q} - m} = -2D^\mu(\not{p} + m) \frac{1}{((p+q)^2 - m^2)^2}, \quad (28)$$

$$\frac{\partial}{\partial q_\mu} \frac{1}{(p+q)^2} = \frac{-2(p+q)^\mu}{(p+q)^4}. \quad (29)$$

This operation gives rise to an additional denominator factor which can be handled, for instance, as follows:

$$\begin{aligned}
& \frac{1}{p_a^2} \frac{1}{p_b^2} \frac{1}{p_c^2} \frac{1}{p_1^2 - m_1^2} \prod_{i=1}^8 \frac{1}{p_i^2 - m_i^2} \\
&= \frac{\partial}{\partial m_1^2} \frac{1}{p_a^2} \frac{1}{p_b^2} \frac{1}{p_c^2} \prod_{i=1}^8 \frac{1}{p_i^2 - m_i^2} \\
&= 11! \int (dz) \frac{z_1}{(\sum_{i=1}^8 z_i (p_i^2 - m_i^2) + z_a (p_a^2 - \lambda^2) + z_b (p_b^2 - \lambda^2) + z_c (p_c^2 - \lambda^2))^{12}}. \quad (30)
\end{aligned}$$

As a consequence, in Eq. (25), $1/V^3$ is replaced by $-1/V^4$, $2!$ is replaced by $3!$, $-2D^\mu$ and $-2(p+q)^\mu$ are multiplied by z_1 , etc., and then everything is multiplied by an overall factor $-q_\lambda$. Recall also that the direction of q is chosen to be opposite to that of p of the lepton line 1. In this manner we obtain

$$\begin{aligned}
\Pi_{LLp}^{\mu\nu}(q) &= -\frac{3!}{2^8} \left(\frac{\alpha}{\pi}\right)^4 \int (dz) (+2z_1 D_1^\mu - 2z_a D_a^\mu - 2z_5 D_5^\mu) \\
&\quad \times \text{Tr} [q(\not{D}_1 + m)\gamma^\alpha(\not{D}_2 + m)\gamma^\beta(\not{D}_3 + m)\gamma^\zeta(\not{D}_4 + m)] \\
&\quad \times \text{Tr} [\gamma^\nu(\not{D}_5 + m)\gamma_\alpha(\not{D}_6 + m)\gamma_\beta(\not{D}_7 + m)\gamma_\zeta(\not{D}_8 + m)] \frac{1}{U^2 V^4}. \quad (31)
\end{aligned}$$

Performing D -operation on $1/V^4$ using Eq. (19), this integral can be expressed in terms of “building blocks” z_i , B_{ij} , A_i , where i, j are indexes for lepton and photon lines. Of course it must be modified by various terms required for renormalization.

C. More on Method C

Let us now consider Method C. In this case it is more convenient to choose the graphic representation in which all three photon lines are parallel (or, uncrossed) in S . Then L can be replaced by a gauge-invariant sum of six light-by-light-scattering diagrams, which we denote as L^μ to indicate that it contains the vertex μ . Similarly R is replaced by R^ν . The explicit form of L^μ of LLp is given by

$$L^\mu = 2[\Pi^{\mu\alpha\beta\zeta}(q, -p_a, -p_b, -p_c) + \Pi^{\mu\beta\zeta\alpha}(q, -p_b, -p_c, -p_a) + \Pi^{\mu\zeta\alpha\beta}(q, -p_c, -p_a, -p_b)], \quad (32)$$

where the light-by-light scattering tensor $\Pi^{\mu\alpha\beta\zeta}(q, -p_a, -p_b, -p_c)$ is defined by

$$\begin{aligned}
\Pi^{\mu\alpha\beta\zeta}(q, -p_a, -p_b, -p_c) &\propto \int d^4l \text{Tr} \left[\gamma^\mu \frac{1}{\not{p}_1 - m} \gamma^\alpha \frac{1}{\not{p}_2 - m} \gamma^\beta \frac{1}{\not{p}_3 - m} \gamma^\zeta \frac{1}{\not{p}_4 - m} \right], \\
p_1 &= l - q, \quad p_2 = l - p_b - p_c, \quad p_3 = l - p_c, \quad p_4 = l, \quad (33)
\end{aligned}$$

with the overall momentum conservation $q = p_a + p_b + p_c$. Actually this procedure gives six identical copies of the original six diagrams so that the result must be divided by 6.

The differentiations in Eq. (16), where $\Pi^{\lambda\sigma}$ is replaced by $(1/6)L^\lambda SR^\sigma$ symbolically, can be carried out as follows:

$$\begin{aligned}
6 \frac{\partial}{\partial q_\mu} \frac{\partial}{\partial q_\nu} \Pi^{\lambda\sigma} &= \frac{\partial^2 L^\lambda}{\partial q_\mu \partial q_\nu} S R^\sigma + \frac{\partial L^\lambda}{\partial q_\nu} \frac{\partial S}{\partial q_\mu} R^\sigma + \frac{\partial L^\lambda}{\partial q_\nu} S \frac{\partial R^\sigma}{\partial q_\mu} \\
&+ \frac{\partial L^\lambda}{\partial q_\mu} \frac{\partial S}{\partial q_\nu} R^\sigma + L^\lambda \frac{\partial^2 S}{\partial q_\mu \partial q_\nu} R^\sigma + L^\lambda \frac{\partial S}{\partial q_\nu} \frac{\partial R^\sigma}{\partial q_\mu} \\
&+ \frac{\partial L^\lambda}{\partial q_\mu} S \frac{\partial R^\sigma}{\partial q_\nu} + L^\lambda \frac{\partial S}{\partial q_\mu} \frac{\partial R^\sigma}{\partial q_\nu} + L^\lambda S \frac{\partial^2 R^\sigma}{\partial q_\mu \partial q_\nu}.
\end{aligned} \tag{34}$$

Although this looks awful, it can be simplified greatly using Ward-Takahashi identities that hold for the gauge-invariant sum L^λ (or R^σ) of light-by-light-scattering diagrams [50]:

$$q_\lambda L^\lambda = 0, \quad q_\sigma R^\sigma = 0. \tag{35}$$

Multiplying Eq. (34) with $q_\lambda q_\sigma$ and applying Eq. (35), we obtain

$$\begin{aligned}
\Pi^{\mu\nu}(q) &= \frac{1}{2} q_\lambda q_\sigma \frac{\partial}{\partial q_\mu} \frac{\partial}{\partial q_\nu} \Pi^{\lambda\sigma}(q), \\
&= \frac{1}{12} \left(\left(q_\lambda \frac{\partial L^\lambda}{\partial q_\nu} \right) S \left(q_\sigma \frac{\partial R^\sigma}{\partial q_\mu} \right) + \left(q_\lambda \frac{\partial L^\lambda}{\partial q_\mu} \right) S \left(q_\sigma \frac{\partial R^\sigma}{\partial q_\nu} \right) \right).
\end{aligned} \tag{36}$$

The great advantage of this equation is that the derivatives like $\frac{\partial L^\lambda}{\partial q_\nu}$ are *UV-finite* so that cut-offs can be safely removed and $\Pi(q^2)$ can be evaluated without renormalization of subdiagram divergences. Of course the overall logarithmic UV divergence must be disposed by charge renormalization.

Eq. (36) provides the starting point of numerical evaluation by Method C. To perform numerical integration, one has to decompose it into non-gauge-invariant forms similar to LLp and LLc . This can be parametrized in the same manner as for Eq. (31), in which light-by-light-scattering diagrams are treated as subdiagrams of the eighth-order vacuum-polarization diagram.

In the following, however, we chose an alternate approach which emphasizes the gauge-invariant nature of the sets L^μ and R^ν of light-by-light-scattering subdiagrams. The set L^μ is a sum of six diagrams in which three photon lines and an external photon line μ are attached to a directed lepton loop in every possible ways. We prepare another set R^ν similarly. We connect them by three photons to construct $L^\mu SR^\nu$. This procedure can also

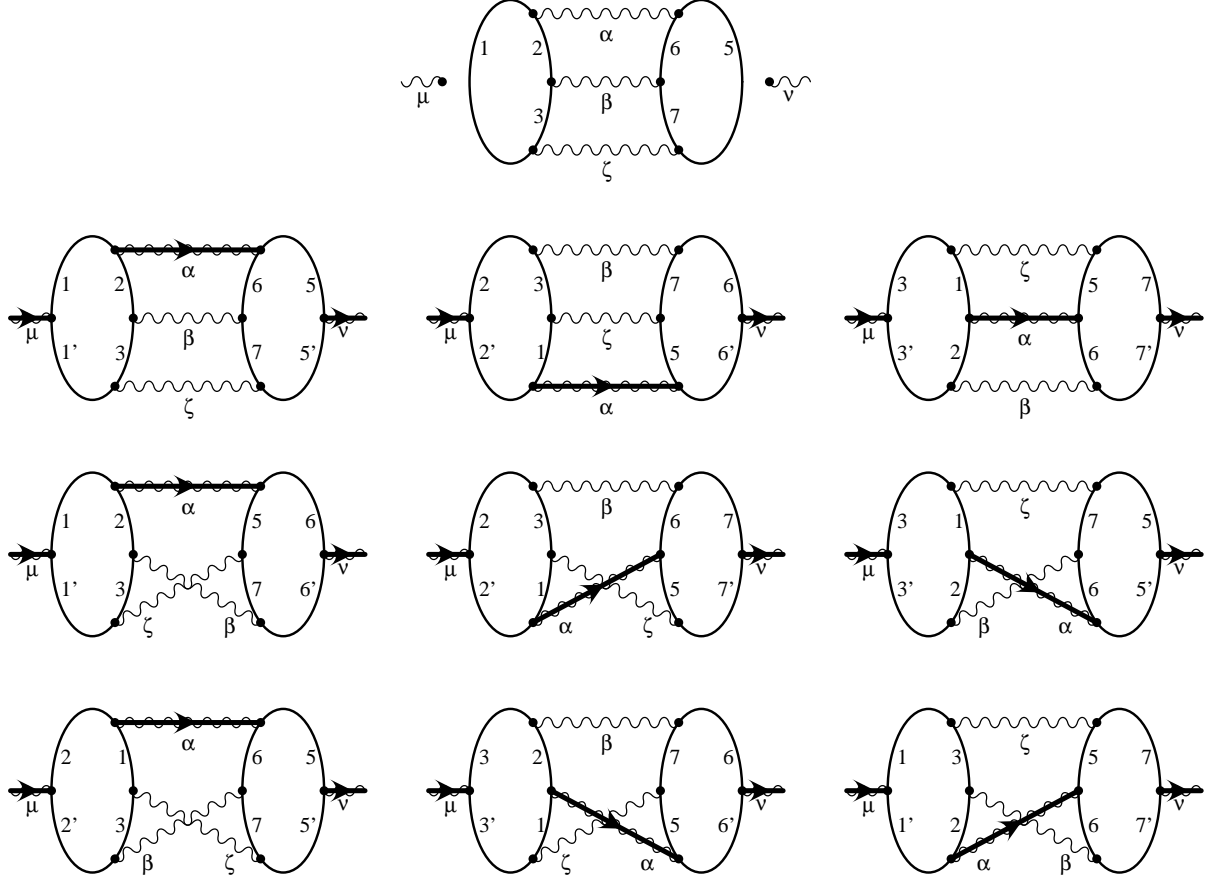


FIG. 3: Diagrams of $L^\mu S R^\nu$. Nine diagrams shown in the bottom three rows are obtained by inserting the external photons labelled μ and ν into the left and right fermion loops, respectively, of the diagram shown at the top. The (bold) internal photon line α carries the momentum q in all cases. Remaining 27 diagrams obtained by flipping the direction of fermion loops are not shown for simplicity.

be stated as follows: suppose there is a diagram with two lepton loops connected by three parallel photons labelled by α, β, ζ from the top to the bottom, and we insert an external vertex μ into the left loop, another external vertex ν into the right loop (see the top figure of Fig. 3). Disregarding the directions of lepton loops for a moment, there are 9 ways of insertions.

It is found that by flipping and twisting the diagrams three of them are topologically equivalent to LLp -type diagram, whose photon lines a, b, c correspond to the cyclic permutations of α, β, ζ , namely, $\{\alpha, \beta, \zeta\}$, $\{\beta, \zeta, \alpha\}$, and $\{\zeta, \alpha, \beta\}$, as shown in the second row of Fig. 3. Similarly, the remaining six diagrams are found to be equivalent to LLc -type,

whose photon lines correspond to all six permutations, namely, $\{\alpha, \beta, \zeta\}$, $\{\alpha, \zeta, \beta\}$, $\{\beta, \alpha, \zeta\}$, $\{\beta, \zeta, \alpha\}$, $\{\zeta, \alpha, \beta\}$, and $\{\zeta, \beta, \alpha\}$, as shown in the third and fourth rows of Fig. 3.

Next we consider the flow of external momentum q in the diagram. Three of four external photon momenta of a light-by-light scattering diagram are independent because of the momentum conservation. L^μ and R^ν in LLp are connected by three photons forming two loops in S . Two of three independent momenta of L^μ thus turn into two loop momenta and can be freely shifted. Therefore, to fix *all* external photon momenta of L^μ and those of R^μ in the $L^\mu SR^\nu$ we need to fix where the only one independent momentum q flows in the entire vacuum-polarization diagram.

We define a fraction of the momentum q_i flowing in the line i , and introduce a coefficient d_i as

$$q_i = d_i q . \quad (37)$$

By momentum conservation, the sum of fractions flowing on three photon lines a , b , and c of S must be equal to 1:

$$d_a + d_b + d_c = 1 . \quad (38)$$

Next we fix the flow of momentum through the gauge-invariant combination $L^\mu SR^\nu$. We consider the following particular choices.

Choice 1: q flows only through the photon line α .

The combination $L^\mu SR^\nu$ is decomposed into LLp -type or LLc -type diagrams listed in Fig. 3, in which q flows only on the photon labelled by α as shown by bold lines. For example, the diagram $\{\alpha, \beta, \zeta\}$ corresponds to the LLp -type diagram in which the fractions are given by $d_a = 1$, and $d_b = d_c = 0$, denoted symbolically as $LLp(d_a = 1)$. Similarly, we can translate all nine diagrams of $L^\mu SR^\nu$ variant to LLp or LLc with specific values of d_i . Then, the gauge-invariant vacuum-polarization function which contains two sets of gauge-invariant light-by-light-scattering subdiagrams is obtained by the combination

$$\begin{aligned} & \frac{4}{6} [\{LLp(d_a = 1) + LLp(d_b = 1) + LLp(d_c = 1)\} \\ & + 2 \{LLc(d_a = 1) + LLc(d_b = 1) + LLc(d_c = 1)\}] , \end{aligned} \quad (39)$$

where it is multiplied by 4 to account for the directions of lepton loops and divided by 6 to take account of duplicated copies.

Once we have selected the flow of q in the photon lines, we can choose any flow on the fermion loops. For instance, we may choose the following flows for three LLp -type diagrams:

diagram with a specific q -flow	fermion 1–4	fermion 5–8
$LLp(d_a = 1)$	$d_1 = -1,$	$d_5 = +1,$
$LLp(d_b = 1)$	$d_1 = d_2 = -1,$	$d_5 = d_6 = +1,$
$LLp(d_c = 1)$	$d_4 = +1,$	$d_8 = -1,$

and other d_i 's are zero. For each diagram, different routings of the external momentum q in the lepton lines is possible, but all give identical results. (This is nothing but a consequence of the “Kirchhoff’s laws” for loops and junctions applied to LLp [45].)

In order to drop the unwanted terms, derivatives of S , second derivatives of L and so on, from Eq. (34), we must add up the contributions from three diagrams in the first line of Eq. (39). To do this, we define the derivative factor $\mathbb{D}^{\mu\nu}$ consisting of two D operators of Eq. (28) as

$$\begin{aligned}\mathbb{D}^{\mu\nu} &\equiv \sum_{\text{three } LLp\text{-type diagrams}} \left(\sum_{i=1}^4 -2d_i z_i D_i^\mu \right) \left(\sum_{j=5}^8 -2d_j z_j D_j^\nu \right) \\ &= 4(-2z_1 z_5 D_1^\mu D_5^\nu - z_1 z_6 D_1^\mu D_6^\nu - z_2 z_5 D_2^\mu D_5^\nu - z_2 z_6 D_2^\mu D_6^\nu - z_4 z_8 D_4^\mu D_8^\nu). \quad (40)\end{aligned}$$

This is derived by a consideration similar to the argument leading to Eq. (31) from the structure of traces implicit in Eq. (36) with the help of Eq. (28). As seen in Fig. 3, $LLp(d_c = 1)$ is in fact identical with $LLp(d_a = 1)$, if the top and bottom of the figure $LLp(d_c = 1)$ is reversed. Thus, we may double the contribution of $LLp(d_a = 1)$ and drop $LLp(d_c = 1)$. Then the coefficient of $z_1 z_5 D_1^\mu D_5^\nu$ becomes -3 and no $z_4 z_8 D_4^\mu D_8^\nu$ term is needed. The vacuum-polarization tensor of LLp -type in Method C is thus given by

$$\begin{aligned}\Pi_{LLp}^{\mu\nu}(q) &= -\frac{4!}{2^8} \frac{4}{6} \left(\frac{\alpha}{\pi} \right)^4 \int (dz) \mathbb{D}^{(\mu,\nu)} \\ &\quad \times \text{Tr} [q(\not{D}_1 + m)\gamma^\alpha(\not{D}_2 + m)\gamma^\beta(\not{D}_3 + m)\gamma^\zeta(\not{D}_4 + m)] \\ &\quad \times \text{Tr} [q(\not{D}_5 + m)\gamma_\alpha(\not{D}_6 + m)\gamma_\beta(\not{D}_7 + m)\gamma_\zeta(\not{D}_8 + m)] \frac{1}{U^2 V^5}. \quad (41)\end{aligned}$$

where the indexes in $\mathbb{D}^{(\mu,\nu)}$ are symmetrized with respect to μ and ν . Eq. (41) is free from UV divergence except for the overall charge renormalization. The Pauli-Villas regularization is no longer required in Eq. (41).

Similarly, we can construct $\mathbb{D}^{\mu\nu}$ factor for LLc :

$$\mathbb{D}^{\mu\nu} = 4(-z_1 z_5 D_1^\mu D_5^\nu + z_1 z_8 D_1^\mu D_8^\nu + z_2 z_8 D_2^\mu D_8^\nu + z_4 z_5 D_4^\mu D_5^\nu + z_4 z_6 D_4^\mu D_6^\nu) . \quad (42)$$

Another simple choice of the q flow is

Choice 2: $\frac{1}{3}q$ flows on all internal photon lines α , β , and ζ .

In this case, all three of LLp - (or six of LLc -) types are indistinguishable. Thus, we find that the gauge-invariant set is

$$\frac{4}{6} \{3LLp(d_a = d_b = d_c = 1/3) + 6LLc(d_a = d_b = d_c = 1/3)\} . \quad (43)$$

The $\mathbb{D}^{\mu\nu}$ operators for LLp and LLc with this choice of q flow can be constructed in the same manner as those in *Choice 1*. The explicit forms of the integrand thus obtained are different between *Choice 1* and *Choice 2*. Hereafter we shall call Method C with *Choice 1* and with *Choice 2* as Method C1 and Method C2, respectively.

The D -operators in Eq. (41), etc., are applied to the V -function on the right-hand side following the “contraction” rules [45]. Carrying out also the trace operations, the result can be written more explicitly in the form

$$\begin{aligned} \Pi_{LLp}(q^2) = \left(\frac{\alpha}{\pi}\right)^4 \int \frac{(dz)}{U^2} \Big\{ & (H_{(1),0} + q^2 H_{(1),1} + (q^2)^2 H_{(1),2} + (q^2)^3 H_{(1),3} + (q^2)^4 H_{(1),4}) \frac{1}{UV^4} \\ & + (H_{(2),0} + q^2 H_{(2),1} + (q^2)^2 H_{(2),2} + (q^2)^3 H_{(2),3}) \frac{1}{U^2 V^3} \\ & + (H_{(3),0} + q^2 H_{(3),1} + (q^2)^2 H_{(3),2}) \frac{1}{U^3 V^2} \\ & + (H_{(4),0} + q^2 H_{(4),1}) \frac{1}{U^4 V} \\ & + \frac{H_{(5),0}}{U^5} \ln \left(\frac{\Lambda}{V} \right) \Big\} , \end{aligned} \quad (44)$$

where the numerators $H_{(r),h}$ are expressed in terms of “building blocks” B_{ij} , z_i , and A_i , $i, j = 1, \dots, 8$ [34, 45] and Λ is the UV cut-off in (21). A detailed structure of $H_{(r),h}$ is presented in Appendix B. The charge renormalization can be trivially carried out, and the cut-off Λ can be put to infinity. We thus obtain the renormalized vacuum-polarization function

$$\bar{\Pi}_{LLp}(q^2) = \lim_{\Lambda \rightarrow \infty} (\Pi_{LLp}(q^2) - \Pi_{LLp}(0)) . \quad (45)$$

It is straightforward to translate Eq. (44) into numerical integration code in FORTRAN by carrying out algebraic manipulation involved with the help of FORM [51].

IV. NUMERICAL RESULTS

We are now ready to describe the numerical evaluation of the contributions of the Set I(j) to the electron $g-2$. The largest contribution, which is mass independent, comes from the case where both fermion loops consist of electrons. We first made a preliminary evaluation of the coefficient of $(\alpha/\pi)^5$ by VEGAS [52] using relatively small sampling points. The results may be summarized as follows:

$$\begin{aligned} A_1^{(10)}(\text{Set I(j): Method B}) &= -0.072\,8843\,8\,(57) + 0.0732\,732\,(118) \\ &= 0.000\,388\,9\,(131), \end{aligned} \tag{46}$$

$$\begin{aligned} A_1^{(10)}(\text{Set I(j): Method C1 } g^{\mu\nu}) &= -0.059\,537\,(39) + 0.059\,917\,(30) \\ &= 0.000\,380\,(50), \end{aligned} \tag{47}$$

$$\begin{aligned} A_1^{(10)}(\text{Set I(j): Method C1 } q^\mu q^\nu) &= -0.0161\,450\,(58) + 0.016\,432\,(161) \\ &= 0.000\,287\,(171), \end{aligned} \tag{48}$$

$$\begin{aligned} A_1^{(10)}(\text{Set I(j): Method C2}) &= -0.047\,895\,3\,(60) + 0.048\,290\,3\,(62) \\ &= 0.000\,395\,0\,(87), \end{aligned} \tag{49}$$

where the first and second terms on the first line of each case are from LLp and LLc respectively. Their vacuum-polarization functions are obtained from the terms proportional to $g^{\mu\nu}$ in Method B, Method C2, and the first Method C1, and the terms proportional to $q^\mu q^\nu$ in the second Method C1. Method B and Method C2 were evaluated on *hp*'s Alpha station. For Method B, we used 10^8 points per iteration and 250 iterations, followed by 10^9 points per iteration and 160 iterations for VEGAS integration. For Method C2, we used 10^8 points per iteration and 100 iterations. Both of Method C1 were carried out with 10^6 points per iteration and 100 iteration on a PC with Intel's Core 2 processor. The Method B requires more sampling statistics for VEGAS than the Method C in order to reduce the uncertainty to the level of the latter, primarily because the renormalization is carried out by point-by-point cancellation between divergent pieces of the integrand. The individual terms of Method B, Method C1, and Method C2 are different from each other because of different treatments of renormalization and routing selection. Note also that the $g^{\mu\nu}$ term and $q^\mu q^\nu$ term in Method C1 give different integrands. The good agreement of these four cases within the numerical uncertainties provides a strong assurance of correctness of all calculations.

method	$g^{\mu\nu}$ or $q^\mu q^\nu$	contribution	sampling points per iteration	iteration
B	$g^{\mu\nu}$	0.000 396 4 (59)	$10^8, 10^{10}$	50, 100
C1	$g^{\mu\nu}$	0.000 398 2 (31)	10^9	101
C1	$q^\mu q^\nu$	0.000 393 8 (88)	10^9	50
C2	$g^{\mu\nu}$	0.000 397 6 (25)	10^9	80

TABLE I: A contribution to the mass-independent term of electron $g-2$, $A_1^{(10)}$, from the diagrams of Set I(j) calculated in various methods. All methods are analytically independent. The overall factor $(\frac{\alpha}{\pi})^5$ is omitted for simplicity. The second column shows from which term, $g^{\mu\nu}$ or $q^\mu q^\nu$ term, the vacuum-polarization function $\Pi(q^2)$ is obtained. The numeral in the parenthesis stands for the uncertainty in the last two digits. All calculations were carried out on RSCC.

The most prominent feature of these calculations is that the LLp and LLc parts are nearly equal in magnitude and almost cancel each other. In view of similar analytic structures of these integrals, this suggests the possibility that cancellation takes place not only between the integrals as a whole but also between the integrands at many points in the domain of integration. If this is the case, one should be able to reduce the calculated uncertainty significantly by performing integration of the combination $2 \times LLp + 4 \times LLc$. In order to verify this conjecture, we have carried out an extensive computation of the combination in both Method B and Method C1.

The production job for evaluation of combined LLp and LLc were carried out on RIKEN's Super Combined Cluster System (RSCC) with 128 or 256 processors. It turns out that the vacuum-polarization functions $\Pi(q^2)$ obtained from $g_{\mu\nu}$ term and $q^\mu q^\nu$ term have analytically different structures in Method C1 and C2 even after combining LLp and LLc . This provides us with more opportunity to check our calculation. The numerical results obtained by various methods are summarized in Table I.

Four values listed in Table I are independent of each other. Thus, combining these results statistically, we obtain

$$A_1^{(10)}(\text{Set I(j): combined}) = 0.000\,397\,5\,(18) \quad (50)$$

as the best estimate of the term $A_1^{(10)}(\text{Set I(j)})$.

loop fermions	$g^{\mu\nu}$ or $q^\mu q^\nu$	contribution	iteration
(e, μ)	$g^{\mu\nu}$	$2.281 (60) \times 10^{-6}$	51
(e, μ)	$q^\mu q^\nu$	$2.290 (115) \times 10^{-6}$	60
(μ, μ)	$g^{\mu\nu}$	$1.185 (17) \times 10^{-7}$	145
(μ, μ)	$q^\mu q^\nu$	$1.284 (4) \times 10^{-7}$	55
(e, τ)	$g^{\mu\nu}$	$1.332 (95) \times 10^{-8}$	100
(e, τ)	$q^\mu q^\nu$	$1.62 (51) \times 10^{-8}$	50
(μ, τ)	$g^{\mu\nu}$	$4.988 (27) \times 10^{-9}$	50
(μ, τ)	$q^\mu q^\nu$	$5.007 (55) \times 10^{-9}$	50
(τ, τ)	$g^{\mu\nu}$	$4.008 (99) \times 10^{-10}$	90
(τ, τ)	$q^\mu q^\nu$	$4.541 (13) \times 10^{-10}$	50

TABLE II: Mass-dependent contributions to the electron $g-2$ from the diagrams of Set I(j) with e , μ and/or τ lepton loops. All integrands are constructed in Method C1. The overall factor $(\frac{\alpha}{\pi})^5$ is omitted for simplicity. The number of sampling points per iteration for VEGAS integration is 10^9 for all calculations. The numeral in the parenthesis stands for the uncertainty in the last two digits. All calculations were conducted on RSCC.

The mass-dependent contributions to the electron $g-2$ involving muons and/or tau leptons are also calculated using the combined programs of Method C1 with $g^{\mu\nu}$ term and with $q^\mu q^\nu$ term. Singular behavior of the integral caused by heavier leptons makes convergence of the integrand rather difficult. But, the contributions themselves are very small and currently of no interest compared with the experimental uncertainty. Therefore we do not need the precise values of the mass-dependent contribution. They are summarized in Table II [53].

Summing up all mass-dependent terms and the mass-independent contribution Eq. (50), we find the total contribution to the electron $g-2$ from Set I(j) given in Eq. (6).

We also present the contributions to the muon $g-2$. They were calculated by replacing the external electron by a muon in the combined program of Method C1 and/or C2. They are listed in Table III. The dominant contribution arises when both of light-by-light scattering loops consist of electrons. Statistically combining three results listed in Table III of this

loop fermions	method	$g^{\mu\nu}$ or $q^\mu q^\nu$	contribution	iteration
(e, e)	C1	$q^\mu q^\nu$	$-1.247\ 28\ (25)$	50
(e, e)	C1	$g^{\mu\nu}$	$-1.247\ 30\ (15)$	71
(e, e)	C2	$g^{\mu\nu}$	$-1.247\ 08\ (31)$	25
(e, μ)	C2	$g^{\mu\nu}$	$-0.016\ 455\ (71)$	20
(e, τ)	C2	$g^{\mu\nu}$	$0.109\ 9\ (51) \times 10^{-3}$	20
(μ, τ)	C2	$g^{\mu\nu}$	$0.149\ 0\ (13) \times 10^{-3}$	20
(τ, τ)	C2	$g^{\mu\nu}$	$0.189\ 3\ (5) \times 10^{-4}$	20

TABLE III: Contributions to the mass-dependent term of muon $g-2$ from the diagrams of Set I(j) with e, μ and/or τ lepton loops. The overall factor $(\frac{\alpha}{\pi})^5$ is omitted for simplicity. The number of sampling points per iteration for VEGAS integration is 10^9 for all calculations. The numeral in the parenthesis stands for the uncertainty in the last two digits. All calculations were carried out on RSCC.

contribution, we found

$$A_2^{(10)}(m_\mu/m_e)(\text{Set I(j)}_{(e,e)} : \text{combined}) = -1.247\ 26\ (12) , \quad (51)$$

where the subscript (e, e) implies that both fermion loops consist of electrons. Including all other contributions, we found the mass-dependent contribution to the muon $g-2$ given in Eq. (7).

V. DISCUSSION

In this paper, we report the evaluation of the contribution to the electron $g-2$ and muon $g-2$ from Set I(j) which consists of six vacuum-polarization diagrams formed by two light-by-light scattering subdiagrams. The contribution to the electron $g-2$ given in Eq. (6) amounts $0.000\ 027 \times 10^{-12}$, which is far smaller than the current experimental uncertainty 0.28×10^{-12} in Eq. (2). Thus far we have no clear explanation of why the contribution from Set I(j) is so small compared with other diagrams of the tenth order.

We have also demonstrated the utility of the Ward-Takahashi identity to deal with the light-by-light scattering subdiagram. Although it may not always help us to streamline the

work-flow for writing numerical programs, we continue to examine its application to the computation of the tenth-order diagrams containing a light-by-light scattering subdiagram that have not been evaluated yet.

Acknowledgments

This work is supported in part by JSPS Grant-in-Aid for Scientific Research (C) 19540322. M. H. is also supported in part by JSPS Grant-in-Aid for Scientific Research (C) 20540261. T. K.'s work is supported by the U. S. National Science Foundation under Grant PHY-0355005. T. K. also thanks for JSPS Invitation Program for Research in Japan S-07165, 2007. Numerical computations were mostly conducted on the RIKEN Super Combined Cluster System (RSCC). A part of preliminary computations was also conducted on the computers of the theoretical particle-physics group (E-ken), Nagoya University.

APPENDIX A: VACUUM-POLARIZATION INSERTION INTO THE ANOMALY INTEGRAL

Analyticity of a vacuum-polarization function $\Pi(q^2)$ ensures that once-subtracted dispersion relation between its real part and imaginary part is given by

$$\frac{\Re\Pi(q^2)}{q^2} = \frac{1}{\pi} \int_0^\infty dk^2 \frac{\Im\Pi(k^2)}{k^2(k^2 - q^2)} . \quad (\text{A1})$$

In the cases of vacuum-polarization of second, fourth, and sixth orders, the cut starts at $q^2 = 4m^2$, where m is the electron mass, and the imaginary part of $\Pi(q^2)$ is nonvanishing for $q^2 > 4m^2$ only. For $\Pi(q^2)$ of Set I(j), however, the cut starts at $q^2 = 0$ because of three photon intermediate states, and is included in Eq. (A1). This is a novel feature encountered for the first time in the eighth-order vacuum polarization. Eq. (A1) also assumes that $\Pi(q^2)$ has no pole at $q^2 = 0$. This may be justified as follows: At the threshold $q^2 = 0$ the absorptive part of $\Pi(q^2)$ is proportional to the square of light-by-light-scattering amplitude, which is proportional to q^8 because the light-by-light amplitude is known to be proportional to q^4 [54]. Meanwhile, three photon propagators could produce $1/q^6$ at most so that $\Im\Pi(q^2)$ behaves as q^2 or even higher positive power of q^2 as $q^2 \rightarrow 0$. Thus the singularity at $q^2 = 0$ cannot be a pole.

Eq. (A1) guarantees that $\Pi(q^2)$ can be expressed by a spectral representation

$$\frac{\Pi(q^2)}{q^2} = \int_0^\infty dk^2 \frac{\rho(k^2)}{-q^2 + k^2}, \quad (\text{A2})$$

where

$$\rho(k^2) = \frac{1}{\pi} \frac{\Im \Pi(k^2)}{k^2}. \quad (\text{A3})$$

The effect of inserting a vacuum-polarization diagram into a photon line with momentum q is thus obtained by replacing the photon propagator by a sum of massive vector propagators whose mass squared is k^2 :

$$\frac{1}{q^2} \longrightarrow \frac{-\Pi(q^2)}{q^2} = \int_0^\infty dk^2 \frac{\rho(k^2)}{q^2 - k^2}. \quad (\text{A4})$$

This is easily translated into a Feynman-parametric integral formula. If a vacuum-polarization is inserted into a photon line z_a , we need to replace a photon mass λ^2 by k^2 , multiply the spectral function $\rho(k^2)$ to the whole integrand, and integrate over a “photon mass” k^2 . This is the most efficient way to describe an effect of the vacuum-polarization insertion in the anomaly calculation.

The spectral function, or the imaginary part of $\Pi(q^2)$, however, is not always available, especially in higher-order cases [43]. On the other hand, we can directly construct $\Pi(q^2)$ itself, or its real part, in the Feynman-parameter space using the Feynman-Dyson rules. Thus our problem becomes how to express the effect of vacuum-polarization insertion by using the real part of $\Pi(q^2)$.

Let us specifically consider the anomaly contribution from a diagram in which a vacuum-polarization diagram is inserted into the second-order vertex diagram. We will omit the overall factor α/π for simplicity and set the electron mass m to unity. It is given as the integral over the Feynman parameters [45]

$$M_{2,P} = \int_0^\infty dk^2 \rho(k^2) \int \frac{(dz)}{U^2} \frac{F_0}{V + z_a k^2}, \quad (\text{A5})$$

where a Feynman parameter assigned to the photon line is z_a and that to the fermion line is z_1 . The explicit form of F_0 , V , \dots , etc. are [45]

$$\begin{aligned} (dz) &= dz_1 dz_a \delta(1 - z_1 - z_a), \quad U = 1, \quad A_1 = 1 - \frac{z_1}{U} \\ F_0 &= z_1 A_1 (1 - A_1), \quad V = z_1 - z_1 A_1 + z_a \lambda^2. \end{aligned} \quad (\text{A6})$$

Comparing Eq. (A5) to Eq. (A2), we find

$$M_{2,P} = \int \frac{(dz)}{U^2} \frac{F_0}{V} (-\Pi(q^2)) \quad (\text{A7})$$

with

$$q^2 = -\frac{V}{z_a} . \quad (\text{A8})$$

Substituting the explicit forms in Eq. (A6) and identifying $z_1 = y$ and $z_a = 1 - y$, one find that Eq. (A7) becomes Eq. (8).

Higher-order diagrams contributing to the magnetic moment may have V^2 or higher powers of V in the denominators. We can easily extend the above method to such cases. Namely, the effect of vacuum-polarization insertion into a photon line z_a is expressed by replacing the denominator $1/V^n$ for $n \geq 1$ according to a following rule:

$$\frac{1}{V^n} \longrightarrow (-1)^n \frac{1}{(n-1)!} \frac{\partial^{n-1}}{\partial V^{n-1}} \left(\frac{\Pi(-V/z_a)}{V} \right) . \quad (\text{A9})$$

This rule is used in our forthcoming papers dealing with the insertion of vacuum-polarization loops in the magnetic moments of fourth, sixth, and eighth orders.

APPENDIX B: STRUCTURE OF THE INTEGRAND OF METHOD C

The integral Eq. (44) generated by Method C is very lengthy containing more than 30,000 terms. The integrand, however, can be shortened by observing its structure carefully. When the term proportional to $g^{\mu\nu}$ is projected out from Eq. (41), D_i^μ and D_j^ν in $\mathbb{D}^{\mu\nu}$ must be “contracted” with other D_k [45]. Knowing it, we can organize $H_{(r),h}$ in the form

$$\begin{aligned} H_{(r),h} = & \sum_{1 \leq k < l \leq 8} T_{(r),h}^{kl} \left\{ \left(\sum_{i=1}^4 d_i z_i B'_{ik} \right) \left(\sum_{j=5}^8 d_j z_j B'_{jl} \right) + (k \leftrightarrow l) \right\} \\ & + F_{(r),h} \sum_{i=1}^4 d_i z_i \sum_{j=5}^8 d_j z_j B_{ij} , \end{aligned} \quad (\text{B1})$$

where $T_{(r),h}$ and $F_{(r),h}$ are expressed in terms of “building blocks” B_{ij} , z_i , and A_i [34]. Then, the number of arithmetic operations is dramatically reduced and the computational time becomes less than one tenth of the program without the above artifice.

[1] P. Kusch and H. M. Foley, Phys. Rev. **72**, 1256 (1947).

- [2] J. S. Schwinger, Phys. Rev. **73**, 416 (1948).
- [3] A. Rich and J. C. Wesley, Rev. Mod. Phys. **44**, 250 (1972).
- [4] R. S. Van Dyck, P. B. Schwinberg, and H. G. Dehmelt, Phys. Rev. Lett. **59**, 26 (1987).
- [5] B. Odom, D. Hanneke, B. D’Urso, and G. Gabrielse, Phys. Rev. Lett. **97**, 030801 (2006).
- [6] D. Hanneke, S. Fogwell, and G. Gabrielse, Phys. Rev. Lett. **100**, 120801 (2008).
- [7] A. Petermann, Helv. Phys. Acta **30**, 407 (1957).
- [8] C. M. Sommerfield, Phys. Rev. **107**, 328 (1957).
- [9] T. Kinoshita, Phys. Rev. Lett. **75**, 4728 (1995).
- [10] S. Laporta and E. Remiddi, Phys. Lett. **B379**, 283 (1996).
- [11] T. Kinoshita and M. Nio, Phys. Rev. D **73**, 013003 (2006).
- [12] T. Aoyama, M. Hayakawa, T. Kinoshita, and M. Nio, Phys. Rev. Lett. **99**, 110406 (2007).
- [13] T. Aoyama, M. Hayakawa, T. Kinoshita, and M. Nio, Phys. Rev. D **77**, 053012 (2008), arXiv:0712.2607.
- [14] M. A. Samuel and G.-w. Li, Phys. Rev. D **44**, 3935 (1991).
- [15] G. Li, R. Mendel, and M. A. Samuel, Phys. Rev. D **47**, 1723 (1993).
- [16] A. Czarnecki and M. Skrzypek, Phys. Lett. **B449**, 354 (1999).
- [17] S. Laporta, Nuovo Cim. **A106**, 675 (1993).
- [18] S. Laporta and E. Remiddi, Phys. Lett. **B301**, 440 (1993).
- [19] B. Lautrup, Phys. Lett. **B69**, 109 (1977).
- [20] M. Passera, Phys. Rev. D **75**, 013002 (2007).
- [21] M. Davier and A. Höcker, Phys. Lett. **B435**, 427 (1998).
- [22] B. Krause (1996), private communication.
- [23] K. Melnikov and A. Vainshtein, Phys. Rev. **D70**, 113006 (2004).
- [24] J. Bijnens and J. Prades, Mod. Phys. Lett. **A22**, 767 (2007), hep-ph/0702170.
- [25] A. Czarnecki, B. Krause, and W. J. Marciano, Phys. Rev. Lett. **76**, 3267 (1996).
- [26] G. Gabrielse, D. Hanneke, T. Kinoshita, M. Nio, and B. Odom, Phys. Rev. Lett. **97**, 030802 (2006).
- [27] G. Gabrielse, D. Hanneke, T. Kinoshita, M. Nio, and B. Odom, Phys. Rev. Lett. **98**, 039902 (2007).
- [28] P. J. Mohr and B. N. Taylor, Rev. Mod. Phys. **77**, 1 (2005).
- [29] P. Cladé et al., Phys. Rev. A. **74**, 052109 (2006).

- [30] A. Wicht et al., Phys. Scr. T **102**, 82 (2002).
- [31] V. Gerginov et al., Phys. Rev. A. **73**, 032504 (2006).
- [32] H. Mueller et al., Phys. Rev. Lett. **100**, 180405 (2008).
- [33] T. Kinoshita and M. Nio, Phys. Rev. D **73**, 053007 (2006).
- [34] T. Aoyama, M. Hayakawa, T. Kinoshita, and M. Nio, Nucl. Phys. B **740**, 138 (2006).
- [35] T. Aoyama, M. Hayakawa, T. Kinoshita, and M. Nio, Nucl. Phys. **B796**, 184 (2008), arXiv:0709.1568.
- [36] T. Kinoshita, T. Aoyama, M. Hayakawa, and M. Nio, Nucl. Phys. Proc. Suppl. **160**, 235 (2006).
- [37] T. Aoyama, M. Hayakawa, T. Kinoshita, and M. Nio, Nucl. Phys. Proc. Suppl. **157**, 106 (2006).
- [38] M. Nio, T. Aoyama, M. Hayakawa, and T. Kinoshita, Nucl. Phys. Proc. Suppl. **169**, 238 (2007).
- [39] T. Aoyama, M. Hayakawa, T. Kinoshita, and M. Nio, PoS (**RAD COR 2007**), 025 (2007).
- [40] T. Kinoshita, Nucl. Phys. Proc. Suppl. **157**, 101 (2006).
- [41] A. H. Hoang, J. H. Kuhn, and T. Teubner, Nucl. Phys. **B452**, 173 (1995), hep-ph/9505262.
- [42] D. J. Broadhurst, A. L. Kataev, and O. V. Tarasov, Phys. Lett. **B298**, 445 (1993), hep-ph/9210255.
- [43] T. Kinoshita and W. B. Lindquist, Phys. Rev. D **27**, 853 (1983).
- [44] T. Kinoshita and W. B. Lindquist, Phys. Rev. D **27**, 867 (1983).
- [45] T. Kinoshita, in *Quantum electrodynamics*, edited by T. Kinoshita (World Scientific, Singapore, 1990), pp. 218–321, (Advanced series on directions in high energy physics, 7).
- [46] D. J. Broadhurst, Z. Phys. **C58**, 339 (1993).
- [47] P. Cvitanović and T. Kinoshita, Phys. Rev. D **10**, 3978 (1974).
- [48] P. Cvitanović and T. Kinoshita, Phys. Rev. D **10**, 3991 (1974).
- [49] R. Karplus and N. M. Kroll, Phys. Rev. **77**, 536 (1950).
- [50] J. Aldins, T. Kinoshita, S. J. Brodsky, and A. J. Dufner, Phys. Rev. D **1**, 2378 (1970).
- [51] J. A. M. Vermaseren (2000), math-ph/0010025.
- [52] G. P. Lepage, J. Comput. Phys. **27**, 192 (1978).
- [53] N. Watanabe, Master’s thesis, Nagoya University (2008).
- [54] H. Euler, Ann. der Phys. **26**, 398 (1936).